8-hydroxy-2'-deoxyguanosine (8-OHdG) biomarker detection down to picoMolar level on a plastic antibody film

Gabriela V. Martins, Ana C. Marques, Elvira Fortunato, M. Goreti F. Sales

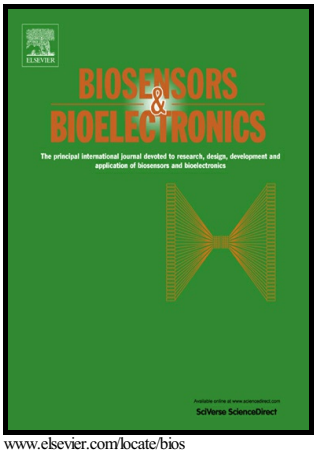

www.elsevier.com/locate/bios

PII: S0956-5663(16)30586-3
DOI: http://dx.doi.org/10.1016/j.bios.2016.06.052
Reference: BIOS8844

To appear in: *Biosensors and Bioelectronic*

Received date: 5 April 2016
Revised date: 1 June 2016
Accepted date: 18 June 2016

Cite this article as: Gabriela V. Martins, Ana C. Marques, Elvira Fortunato and M. Goreti F. Sales, 8-hydroxy-2'-deoxyguanosine (8-OHdG) biomarker detection down to picoMolar level on a plastic antibody film, *Biosensors and Bioelectronic,* http://dx.doi.org/10.1016/j.bios.2016.06.052

8-hydroxy-2'-deoxyguanosine (8-OHdG) biomarker detection down to picoMolar level on a plastic antibody film

Gabriela V. Martins[1,2], Ana C. Marques[2], Elvira Fortunato[2], M. Goreti F. Sales[1,*]

[1)]BioMark/CINTESIS-ISEP, School of Engineering of the Polytechnique School of Porto, 4200-072 Porto, Portugal

[2)] i3N/CENIMAT, Department of Materials Science, Faculty of Science and Technology, Universidade NOVA de Lisboa and CEMOP/UNINOVA, Campus de Caparica, 2829-516 Caparica, Portugal

To whom correspondence should be addressed: Goreti Sales, School of Engineering of the Polytechnique School of Porto, R. Dr. António Bernardino de Almeida, 431, 4200-072 Porto, Portugal. Tel: +351228340544; Fax: +351228321159. goreti.sales@gmail.com; mgf@isep.ipp.pt.

Abstract

An innovative biosensor assembly relying on a simple and straightforward *in-situ* construction is presented to monitor urinary 8-hydroxy-2'-deoxyguanosine (8-OHdG) down to the pmol/L level. The sensing film of the biosensor consisted of a molecularly imprinted polymer (MIP) layer for 8-OHdG assembled on a gold electrode through electropolymerization of monomer combined with the template.

The analytical features of the resulting biosensor were assessed by Cyclic Voltammetry (CV) and Electrochemical Impedance Spectroscopy (EIS). Some experimental parameters such as the initial concentration of the monomer and the ratio template-monomer were investigated and optimized in order to finely tune the performance of the MIP-based sensor. Under optimal conditions, the developed biosensor was able to rebind 8-OHdGwith a linear response against EIS from 0.1 to 100

pg/ml (3.5 to 3500 pM). The interference of coexisting species was tested, also with calibrations on urine samples, and good selectivity towards 8-OHdG was obtained.

RAMAN spectroscopy, FTIR and SEM evaluations of the prepared films confirmed the formation of a polyphenol thin-film on the electrode surface. The presence and distribution of the imprinted cavities on the MIP layer was confirmed by confocal microscopy imaging of the film, after a post-treatment with Fluorescein Isothiocyanate (FITC) labeled 8-OHdG antibody.

Overall, this label-free biosensor for urinary 8-OHdG detection constitutes a promising low-cost alternative to the conventional immunoassay approaches, due to its simplicity, stability, high sensitivity and selectivity for biological sample assays, opening new doors for other applications.

Keywords: 8-hydroxy-2'-deoxyguanosine; molecularly imprinted polymer; electropolymerization; electrochemical biosensor; urine biomarker.

1. Introduction

In living aerobic organisms, excessive production of Reactive Oxygen Species (ROS) is widely recognized as a central feature of many biological processes and diseases due to their impact on cell injury and consequently death. ROS formation is involved in aging, neurodegenerative diseases such as, Alzheimer, Parkinson and Huntington disease, and also cancer (Repine et al., 1997)(de Zwart et al., 1999). Likewise, chronic and accumulative Oxidative Stress (OS) induces damaging modifications to a variety of biomolecules including DNA, lipids and proteins. In this context, the formation of 8-hydroxy-2'-deoxyguanosine (8-OHdG) through DNA hydroxylation is an important mechanism of oxygen-radical induced mutagenesis (Valavanidis et al., 2009). 8-OHdG is a repair product of oxidized guanine lesions and has been acknowledged as a suitable biomarker of OS (Kasai, 1997). Moreover, a correlation has already been established between an increase in OS levels and carcinogenesis (Frenkel, 1992).

Despite all the research efforts that have been made in the last decades, early detection is still the most crucial determinant for successful cancer treatment and survival. Thus, the demand for OS biomarker assays carried out in wide screening programs in *point-of-care* is critical. Consequently, 8-OHdG biomolecule has been quantified in various biological samples, such as, urine (Lee et al., 2010)(Subash et al., 2010)(J. C. Wang et al., 2014), saliva (Guan et al., 2014), blood (Bolner et al., 2011) and tissue (Arnett et al., 2005). It was found that the average levels of 8-OHdG in healthy humans is around 20 ng/ml, a value that increases when OS rises (Richard G. Cutler, 2002). Bolner *et al.* have demonstrated that 8-OHdG levels in Parkinson's disease patients can be 2-3 times higher than in healthy controls (Bolner et al., 2011). Thus, highly sensitive (nanomolar level) methodologies are needed for the assessment of 8-OHdG.

Various methods have been proposed to analyze 8-OHdG in biological samples, including Resonance Rayleigh Scattering (*RRS*) (Guo et al., 2012), Gas Chromatography - Mass Spectrometry (*GC-MS*) (Mei et al., 2005), Enzyme-Linked Immunosorbant assay (*ELISA*) (Yano et al., 2009) and High Performance Liquid Chromatography (*HPLC*) (Kasai, 1997). Although these conventional detection techniques have reached good selectivity and suitable detection limits, these are time consuming and often require the use of sophisticated and laborious technologies, highly qualified personnel, and excessive handling of biological samples. So, the development of fast, sensitive, easy-to-use and low cost methods for 8-OHdG detection remains a challenge.

As alternative to these conventional approaches, few biosensing devices have been reported in the literature, relying mostly on electrochemical or Quartz Crystal Microbalance (*QCM*) detection modes. Such devices establish a direct reading of 8-OHdG, making use of its active redox properties on glassy carbon (Gutiérrez et al., 2016)(Jia et al., 2015)(L. Jia et al., 2013)(L. Yang et al., 2015) or pyrolytic graphitic (Gupta et al., 2016) supports, modified with highly conductive nanomaterials of multi-wall carbon nanotubes or graphene. In general, the detection capability of these devices varies from 1.1 to 97 nM, but some methods have shown severe interference from urine elements (mostly

uric acid), solved therein by the addition of specific enzyme prior to the analysis stage. The use of antibodies as biorecognition element attached to gold supports (N. S. Ferreira & Sales, 2014), graphitic surfaces (Tehrani et al., 2014) or silicon nanowires (Mohd Azmi et al., 2014), has solved such lack of selectivity problem. The inherent devices also offered simplicity of construction and good detection features, varying from 0.35 to 7.1 nM. However, as antibodies are proteins in nature, the corresponding devices may hold limited stability and reproducibility features.

As an alternative recognition element in electrochemical biosensors, plastic antibodies may bring out new advantages to 8-OHdG detection. These synthetic materials are obtained by molecularly-imprinted technology and are linked to longer stability properties and lower production costs than their natural counterparts. In this context, and as far as we know, a single approach has been presented in the literature targeting 8-OHdG. It consisted in creating imprinted sensing films using metal chelating agents (used as monomers) cross-linked with bisacrylamide (Say et al., 2009). The affinity features of these materials towards 8-OHdG were measured by QCM gold sensing receptor surfaces, but the detection capabilities were not lower than 0.01 μM. In addition, such materials have been reported in 2008-2009, and since then significant developments on molecular-imprinting technology have been addressed in the literature.

Molecular imprinting technology has become today an important tool to design nanostructured materials with highly tunable recognition properties. Briefly, molecularly imprinted polymers (MIP) are synthetic polymers holding specific recognition sites that are complementary in size, shape and functional groups to the target molecule (Malitesta et al., 2012). In particular, MIP approach has arise from the need to achieve facile, robust and cost effective alternative methods. Currently, MIPs offer a wide range of applications including drug delivery systems (Barde et al., 2012)(Alvarez-Lorenzo & Concheiro, 2004), stationary phases (Vallano & Remcho, 2000)(Sahebnasagh et al., 2014), solid phase extraction (Sahebnasagh et al., 2014)(Owens et al., 1999) and biosensing devices (Whitcombe et al., 2011)(Moreira et al., 2013). In recent years, the high stability and specificity of

MIPs have turned these promising alternative to immunosensors. Furthermore, different detection mechanisms such as, Surface Plasmon Resonance (*SPR*) (Pernites et al., 2011), Voltammetry (Moreira et al., 2013), Electrochemical Impedance Spectroscopy (*EIS*) (Panasyuk et al., 1999) and fluorescence quenching (Nguyen & Ansell, 2009) have been used in MIP-based chemical sensors. The integration of the imprinting approach with electrochemical sensing technique has enhanced both the sensitivity and selectivity of the sensors (Li et al., 2013).

In the field of biosensors, the main feature concerning the assembling of MIP is the proper integration between transducer and recognition elements. In this sense, electropolymerization approach enables the formation of selective binding sites, at a precise spot, closer to the electrode surface. By controlling the polymerization parameters (applied voltage, charge, number of cycles, supporting electrolyte, etc.), it becomes possible to precisely tune the rate of polymer growth, the film thickness and their morphological characteristics (Sharma et al., 2012). One of the main advantages of using the electropolymerization technique is the ability to carry out MIP synthesis and biomolecule immobilization in a one-step procedure. Furthermore, electrochemistry is a simple, low cost and quite sensitive tool, easily applied to electroactive species in aqueous media. Recently, a MIP sensor for dopamine detection based on a chitosan-graphene mixture have demonstrated how bulk imprinting of small size molecules can be a simple and successfull approach (Liu et al., 2012)(Y. Yang et al., 2011). In addition, carbon nanotubes and supramolecular cyclodextrins have been chosen to modify electrodes for simultaneous determination of DNA bases (Shen & Wang, 2009). Over the last decade, the use of MIPs as recognition elements towards the assessment of biological molecules was constantly reviewed, specifically, the effect of experimental conditions including pH, nature of the buffer and charges/ functional groups has been investigated (Kamel et al., 2008)(Gutiérrez et al., 2008)(Luo et al., 2014). Herein, special emphasis has been given to electropolymerization of phenol for the preparation of MIP-based sensors, due to its straightforward

preparation and its ability to interact with different analytes, through hydrogen bonding and π-π stacking (Riskin et al., 2007)(Malitesta et al., 2012).

In the present work, a simple and sensitive electrochemical MIP-based sensor for detection of urinary 8-OHdG has been assembled via electropolymerization. To this end, 8-OHdG was employed as the template molecule and phenol as the functional monomer (see Figure 1). One of the main advantages of the application of polyphenol films is their facile preparation by electropolymerization in mild aqueous media suitable for biological molecules. Several experimental parameters have been carefully optimized and the electrochemical performance of the designed MIP sensor was investigated by Cyclic Voltammetry (CV) and Electrochemical Impedance Spectroscopy (EIS). Moreover, it was employed to detect 8-OHdG in urine samples as a non-invasive approach to assess the extent of DNA oxidative damage. Thus, the proposed biosensor provides a highly selective tool to be implemented as an easy-to-use protocol for sensitive detection of 8-OHdG in biological samples.

2. Experimental

2.1 Reagents and Materials

All chemicals were of analytical grade and used as supplied without further purification. All buffer solutions were prepared in phosphate buffered saline (PBS, 0.01 M, pH 7.4) with ultrapure water Mili-Q laboratory grade. The exact pH values were measured with a pH meter (Crison Instruments, GLP 21 model). Potassium hexacyanoferrate III ($K_3[Fe(CN)_6]$) and potassium hexacyanoferrate II ($K_4[Fe(CN)_6]$) trihydrate were obtained from Riedel-de-Haen; 3-mercapto-1-hexanol, phenol (for molecular biology) and 8-hydroxy-2-deoxyguanosine (8-OHdG, 98%) from Sigma-Aldrich; ethanol absolut (99.8%) from Panreac and the Fluorescein Isothiocyanate (FITC) labeled antibody against 8-OHdG (polyclonal, 100 μg, 0.5 mg/ml in PBS) from Biorbyt. Piranha solution was prepared by

carefully mixing concentrated sulfuric acid (H_2SO_4, 95%, Normapur) and hydrogen peroxide (H_2O_2, 30%, Scharlau) in 5:1 ratio. All experiments were carried out at ambient temperature.

2.2 Apparatus

Electrochemical measurements were performed by using a classical three-electrode system consisting of a gold-modified electrode as the working electrode, a platinum wire as the counter electrode and a Ag/AgCl wire as the reference electrode. The diameter of the working electrode was 2 mm. The electrochemical measurements were conducted with a potentiostat/ galvanostat from Metrohm Autolab and a PGSTAT302N with a FRA module, controlled by ANOVA software.

Fourier Transform Infrared Spectroscopy (FTIR), Raman spectroscopy and Scanning Electron Microscopy (SEM) characterization was conducted using gold-screen printed electrodes (Au-SPE) purchased to DropSens (DRP-220AT), instead of the conventional gold electrode. FTIR measurements were performed using a Thermo Scientic Smart iTR Nicolet iS10, coupled to the Attenuated Total Reflectance (ATR) smart accessory, also from Thermo Scientific. For Raman analysis, we have used a Thermo Scientific DXR Raman microscope system with a 100 mW 532 nm excitation laser. For both FTIR and RAMAN measurements, data analysis was performed with OMNIC software. Surface morphology of the polymeric films was examined in a Carl Zeiss AURIGA Crossbeam SEM-FIB workstation.

The images concerning MIP and NIP labeled with FITC-anti-8-OHdG were collected by a Confocal Laser Scanning Microscope (LSM 700/ Carl Zeiss). Afterwards, the image analysis was performed using ZEN 2.1 software (Carl Zeiss).

2.3 Gold electrode cleaning

Before use, the bare gold electrode was cleaned by dipping in a mixture of piranha solution for 20 min, rinsing abundantly with ultra-pure water and drying. Then, the electrode was carefully polished

with aqueous alumina slurries, with successive decrease in particle size (1–0.05 μm), followed by sonication in ethanol-water mixture. Finally, the electrode was abundantly washed with ultra-pure water and allowed to dry at ambient temperature. Before each experiment, the electrode was subjected to cyclic sweeping between –0.2 and 1.5 V, in 0.5 M H_2SO_4 solution, until a stable cyclic voltammogram was obtained (more or less 5 cycles).

2.4 Sensor fabrication

Initially, the gold (Au) surface of the electrodes was modified with a monolayer of 3-mercapto-1-hexanol. The clean Au electrode was immersed in a 20 mM thiol solution for 2 hours, at 25ºC, in order to form the covalent attachment of thiol to the Au electrode surface. This incubation step was responsible for the formation of a stable self-assembled monolayer on the electrode surface through a strong gold-sulfur interaction.

MIPs were prepared by bulk polymerization and all experiments were carried out at ambient temperature. Previously, the phenol solution was deoxygenated by bubbling nitrogen gas for 15 min. Afterwards, the electropolymerization was performed by CV (3 cycles) in the potential range +0.1 to 0.9 V, at a scan rate of 20 mVs^{-1}, in a 0.01 M PBS solution, containing both phenol monomer and the template molecule 8-OHdG. MIP solutions were renewed every 3 experiments. Then, template removal was carried out by consecutive immersion in ethanol and PBS solutions, for 30 min each, leading to the formation of recognition cavities in the MIP structure. This solvent was chosen to ensure an efficient removal of 8-OHdG, while keeping mild conditions and avoiding pH changes upon the polymeric film.

Control electrodes (NIPs or non-imprinted polymer) were prepared by following the same procedure but without the presence of the template molecule. The NIP electrode had the same treatment as the MIP sensor, in order to ensure that variations were only attributed to the imprinting features. All the modified electrodes were stored at 4ºC before further use.

2.5 Electrochemical assays

Electrochemical measurements for characterization of the modified electrodes were performed by using different electrochemical techniques, such as, Cyclic Voltammetry (CV) and Electrochemical Impedance Spectroscopy (EIS]. For CV assays, the potential was scanned from –0.1 to +0.4 V, at 50 mVs^{-1}, in 5.0×10^{-3} mol/L $K_3[Fe(CN)_6]$ and $K_4[Fe(CN)_6]$, in 0.01 M PBS solution, pH 7.4. EIS assays were conducted with the same redox couple $[Fe(CN)_6]^{3-/4-}$, at a standard potential of +0.15 V, with a number of frequencies equal to 50, logarithmically distributed over a frequency range 10^{-3}-10^{4} Hz. All experiments were conducted in triplicate at ambient temperature.

Calibration curves were made with 8-OHdG standard solutions ranging from 0.10 and 100.0 pg/mL. All standard solutions were freshly prepared in PBS pH 7.4. The time given for 8-OHdG incubation before reading of the redox probe was set to 20 min.

2.6 Surface analysis

Each step of chemical modification on the gold electrode was followed *ex-situ* by FTIR, Raman and SEM analysis. For this purpose, the polymeric films were grown on Au-SPE for 10 CV cycles. Before measurement, samples were left drying at room temperature, for at least one day. Regarding FTIR analysis, the infrared spectra were collected after background correction, with a number of scans set to 500. Raman spectra were recorded using a 4 mW power, exposure time 60 s, number of exposures 10 and 50 μm slit aperture. SEM images were obtained by using an accelerating voltage of 5 kV with an aperture size of 30 μm.

2.7 Preparation and characterization of the FITC-labeled surfaces

Fluorescence microscopy was employed to assess the presence and distribution of the rebound 8-OHdG molecule via fluorescent emission from the FITC labeled antibody. The fluorescence studies

were conducted on MIP and NIP surfaces built on Au-SPE. Afterwards, the rebinding of 8-OHdG molecule was performed in the same conditions of the calibration procedure. The antibody was previously diluted 1:100 in PBS and incubated on top of the electrodes for one hour (4ºC). All the fluorescence measurements were carried out with the excitation wavelength of 488 nm and the emission wavelength of 520 nm. Control images of non-imprinted electrodes were obtained in identical experimental parameters. Afterwards, all images were processed in equal conditions, by applying a brightness filter of 80% and a contrast filter of 90% in order to improve fluorescence visualization.

2.8 Selectivity studies and analysis in urine samples

The selectivity experiments were carried out through incubation of the MIP-based sensor in 8-OHdG solution (5 pg/ml) in the presence of each individual interfering species. Uric acid, citric acid and glucose were chosen as interfering molecules and used at concentrations mimicking the physiological levels. In addition, selectivity features of the MIP were assessed directly in human urine samples, due to their complex nature as a biological fluid. The urine samples were collected in sterile bottles to avoid any contamination. After collection, the fresh urine samples were directly frozen in aliquots of 1 mL. Before analysis, the samples were diluted in PBS buffer, in a 1:1000 ratio.

The detection analysis of 8-OHdG in urine samples was tested by immersing the MIP sensor in the diluted samples during a period of incubation of 20 min, followed by EIS analysis. Preliminary recovery tests were performed by adding a known concentration of 8-OHdG to urine samples.

3. Results and Discussion

3.1 Optimization of experimental variables

During the fabrication of MIP materials, several parameters need to be carefully optimized. Herein, the concentration of monomer, the number of CV cycles and its ratio against the target analyte have been considered, as these are found critical steps at the MIP film assembly (Huang et al., 2011)(Gohary et al., 2014)(Yola et al., 2015)(Liu et al., 2012). The pH was also a very important parameter, but it was kept at this stage equal to 7.4, as this is a close condition to that in biological fluids.

The electropolymerization of phenol was achieved by CV. Figure 2A illustrates the first voltammetric cycle concerning the electropolymerization of phenol, at pH 7.4, for different concentrations of monomer. As shown, pure phenol solutions exhibited only an oxidation peak around +0.6 V, indicating an irreversible oxidation reaction of the monomer on the electrode surface. It was clear that the peak current increased with increasing monomer concentration 0.25 < 0.50 < 1.25 mM. Due to the non-conductive behaviour of polyphenol (Sharma et al., 2012), this accounted the growth of a strongly passivating polymer layer on the electrode surface. In general, a great increase in the overall resistance of the sensing layer may hinder the sensitivity of the device. On the other hand, for concentrations of monomer below 0.25 mM, the efficiency of the polymerization reaction may be small, questioning the stability of the polymeric film. Therefore, 0.25 mM was identified as the optimum phenol concentration for the preparation of the 8-OHdG sensor.

Another challenge within the MIP technology is to find an agreement regarding the concentration and distribution of recognition sites close to the sensor surface and, simultaneously, well connected along it (Blanco-López et al., 2003). Likewise, the number of cycles during the electropolymerization of the monomer can tailor both the thickness and structural characteristics of the resulting polymeric film (Ferreira et al., 2006). In our investigations, no more than 3 voltammetric cycles were used during the electropolymerization of phenol to avoid that 8-OHdG molecules could be buried deep within the polymeric film, inhibiting their subsequent elution in

order to create effective recognition sites. In addition, a higher number of cycles would generate a less conductive surface and, subsequently, a less sensitive device.

Next, the effect of the mole ratio of 8-OHdG molecule to phenol monomer was also investigated. Figure 2B presents the time-dependent charge response during electropolymerization of NIP films and MIP films with different ratios of template/monomer (1:3 and 1:1). The thickness of the polymer film can be roughly estimated from the total charge during electropolymerization (Panasyuk et al., 1999). According to Figure 2B, the total charge resulting from phenol electro-oxidation in the NIP is around 2×10^{-4} C and, therefore, the thickness of the polymeric film was about ~60 nm. This result is in agreement with previous studies performed in similar conditions (Z. Wang et al., 2007) (M. Ferreira et al., 2006). Different ratios of template to monomer were investigated for the MIP material, in order to optimize the amount of binding sites available for the selective re-binding of 8-OHdG. When the ratio was 1:3, the charge response decreased comparatively with NIP, as shown in Figure 2B, while in the case of a ratio 1:1, the charge response increased again. So, although our results have showed that the presence of the target analyte affects the total charge resulting from phenol oxidation, the previous approach used to estimate the thickness of the films can only be applied to the polymer layer. Overall, the presence of the target molecule within the film hindered the growing of the polymer, as it did not participate in the polymerization stage. In addition, calibration curves of 8-OHdG in PBS solution at pH of 7.4 were performed for both MIPs and the highest electrochemical response (highest sensitivity) was obtained for the MIP with the ratio template to monomer of 1:1 (Figure S1 in supplementary data). Thus, the optimal template-monomer ratio of 1:1 was chosen for the following studies expressing a final concentration of imprinted molecule of 75 μg/ml.

3.2 Preparation and electrical follow-up of MIP sensor

Figure 2C shows a typical voltammogram recorded during the electropolymerization of phenol in the presence (dashed line) and absence (solid line) of 8-OHdG. The only peak visible occurred around +0.6 V and is due to phenol oxidation. This record also indicated that 8-OHdG was not electroactive in the range 0.1–0.9 V, meaning that the template structure was not electrochemically altered and was preserved during the imprinting step. Furthermore, it was clear that the current decreased with increasing number of cycles and the highest current was obtained in the 1st cycle. As expected, after the 2nd and 3rd cycles, the phenol oxidation peak started to disappear, which resulted from the formation of a non-conductive layer that blocked the access of the monomers to the electrode surface. It was interesting to see that the peak current in the presence of 8-OHdG was smaller than that obtained without it, which can be a strong indication of the existing interactions between the phenol monomer and the template molecule. The hydroxyl groups in the 8-OHdG molecule could be interacting with the phenol monomer through hydrogen bonding. This is consistent with several other reports that have confirmed the importance of electrostatic interactions and hydrogen bonding between template molecules and phenol (Yola et al., 2015)(Guo et al., 2012). Recently, the construction of graphene-based MIPs have supported that hydrogen bonds between template and polymeric matrix can enhance the recognition and selectivity for the target molecule (Luo et al., 2014). Moreover, previous studies have demonstrated that π donor-acceptor interactions between electropolymerized phenol and an imprinted template molecule can be used as a novel method to generate imprinted polymers (Riskin et al., 2007).

The construction of NIP and MIP sensors was followed *in-situ* by CV and EIS measurements in 5 mM $[Fe(CN)_6]^{3-/4-}$ solution, prepared in 0.01 M PBS as the supporting electrolyte. Figure 3A shows the cyclic voltamogramms obtained with gold-modified electrodes, where a couple of well-defined redox peaks was evidenced, as a result of the reversible electron transfer of the redox pair $[Fe(CN)_6]^{3-/4-}$. After pre-incubation of thiol onto the gold surface, the current of the redox peak observed decreased, meaning that this modification slightly increased the electrical resistance of the

working electrode. This outcome was expected as the result of the spontaneous formation of a closely packed monolayer via a strong gold-sulphur interaction between the −SH group and the gold. Afterwards, it was found that the formation of polyphenol polymeric layer hindered the electron transfer process resulting in a good blocking efficiency on the electrode surface. Thus, the NIP and MIP formation are characterized by the disappearance of the pair of redox peaks (Z. Wang et al., 2007). Interestingly, the MIP film showed lower current change throughout the voltammogram in comparison to the NIP, which was a strong evidence of the presence of the template 8-OHdG within the polymer matrix. Once the template was extracted from the MIP, the film recovered some of the current change lost, accounting the exit of the imprinted template from the polymer matrix and thereby confirming the formation of binding sites. As expected, after the 8-OHdG removal step (with ethanol-PBS solutions), the electrochemical behaviour of the NIP was unaltered.

EIS studies were used to follow-up the variation of gold-modified electrodes after each chemical change, since this electrochemical measurement holds a high sensitivity and it is strongly suitable in the detection/follow-up of small alterations of non-conductive polymers. Randle's equivalent circuit was adopted to model the physiochemical process occurring at the gold electrode surface. In general, the impedance spectra included a semi-circular portion at higher frequencies and a linear portion at lower frequencies which corresponded to the electron-transfer resistance and the diffusion process, respectively. The diameter of this semicircle is the charge-transfer resistance (R_{ct}) that controls the electron transfer kinetics of the redox-probe at the electrode interface. Figure 3B illustrates the Nyquist diagrams of the electrodes fabricated at each step in the presence of 5 mM $[Fe(CN)_6]^{3-}$ /$[Fe(CN)_6]^{4-}$, which were carried out at the formal potential of 0.15 V with a frequency range of 10000 to 0.001 Hz. The bare gold surface presented a small semicircle domain as the result of a very fast electron-transfer process (Figure 3B-a). Afterwards, the modification with the thiol monolayer onto the gold surface gave rise to a subsequent increase in R_{ct} (Figure 3B-b). As expected, the electropolymerization of phenol resulted in a substantial increase of impedance (Figure 3B-c) due to

the blocking of electron transfer by the polymeric matrix. Furthermore, a higher increase of the impedance was observed when the polymerization of phenol took place in the presence of 8-OHdG (Figure 3B-e), accounting the presence of 8-OHdG entrapped inside the polymeric matrix (consistent with the fact that the addition of 8-OHdG promotes an R_{ct} increase, evidenced in Figure S1. Finally, the elution of the template from the polymer matrix is acknowledged as one of the most important steps, since it holds a direct influence on the sensitivity to the template recognition. Previous studies with other small template molecules, like 8-OHdG, have performed the removal of these molecules from the MIP structure by extraction with PBS or ethanol solutions (Huang et al., 2011)(Liu et al., 2012). For instance, a capacitive sensor developed by electropolymerization of phenol has achieved theophyline template elution via aqueous-ethanol mixtures (Z. Wang et al., 2007). Herein, the removal of the template was achieved by incubating the MIP film in ethanol and PBS. This procedure has led to a substantial R_{ct} decrease of the MIP film (Figure 3B-f), accounting the formation of imprinted cavities that facilitate the diffusion of $Fe(CN)_6^{3-/4-}$ through the polymer network. The same treatment applied to the NIP film has generated only a slight R_{ct} reduction, correlated to the washout of unreacted monomer or small oligomers (Figure 3B-d). Thus, it seems evident that the huge R_{ct} decrease at the MIP layer is mostly linked to the successful exit of the target template from the polymeric material.

3.3 Characterization of the modified surfaces

FTIR and RAMAN measurements were conducted in order to verify each chemical modification step along the sensor assembly, specifically, the formation of polymeric films produced by electro-oxidation of 0.25 mM phenol in PBS solution. In both assays, the analysis was performed directly on a gold-screen printed electrode (Au-SPE). Figure 4 shows the FTIR-ATR and Raman spectra of bare Au, the thiol modification, and NIP and MIP films assembled on the working electrode area.

Regarding the FTIR data, the assembling of a thiol layer on the gold surface was confirmed by the appearance of a well define band around 1100 cm^{-1} that could be attributed to the stretching vibration of the C–O bound (Lapuente et al., 1998). The formation of the polymeric layer of polyphenol was confirmed by the broad band associated with the aromatic out-of-plane C–H deformation vibrations in the range 750-650 cm^{-1} (only visible in NIP and MIP spectra) (Socrates, 2004). No differences could be verified on the FTIR spectra of NIP and MIP materials, but this was consistent with the fact that their main chemical composition was the same.

The RAMAN spectra of the Au-SPE showed 3 bands at 500, 550 and 830 cm^{-1} that could be assigned to carbon compounds that are present in the manufacturing of the gold ink paste. Comparison between Au-SPE and thiol-modified spectra showed a substantial reduction in the intensity of the 830 cm^{-1} peak as the result of the assembling of a monolayer of thiol, thus covering the gold surface. Spectra of NIP and MIP films produced over the Au-modified-SPEs presented a significant increase of the Raman shift at 500 and 550 cm^{-1}, that could be attributed to the aromatic ring deformation, confirming the growth of the polymeric chain. Interestingly, the two broad undefined bands around 1500 and 2900 cm^{-1} are probably a strong indication of surface modification due to polymerization, as these are expected to be related with the emission of fluorescence coming from the aromatic rings.

Surface morphology of the prepared NIP and MIP electrodes was further studied by means of SEM. From figure 5A, we verified that the formation of the phenol polymer seems to be well distributed/spread on the surface. As expected, due to the small dimension of 8-OHdG molecule, it was impossible to visualize the imprinted cavities but, interestingly, MIP surface seems to hold a more globular morphology, with more islets, compared with the NIP one. Moreover, the comparison between NIP and MIP images have showed that the MIP surface presents a higher porosity than NIP. This different behaviour in the polymer morphology can be another strong indication that the

presence of 8-OHdG molecule during electropolymerization resulted in a different structural polymeric growth.

Previous studies have reported the design and development of aqueous phase molecular imprinting coupled to confocal microscopy imaging, aiming to visualize the imprinting effect (Hawkins et al., 2006). Herein, we have followed the binding of a FITC labelled antibody targeted against 8-OHdG to the surface of the sensor in order to track the 8-OHdG oxidative stress biomarker rebound into the imprinted cavities. Figure 5B presents confocal micrograph images of FITC-labelled antibody 8-OHdG on the electrode surfaces. The well-localized fluorescence signals present on MIP sample indicated that the FITC labelled antibody have selectively bound to the target molecule. Moreover, fluorescence signal points were localized in a homogeneous manner only on the MIP electrode, which is strong evidence that the target molecule was rebound and, consequently, imprinted cavities have been successfully created. In parallel, the image of a non-imprinted polymer control taken at identical experimental parameters presents a distinct lack of a homogeneous distribution of fluorescence. Furthermore, our findings also confirmed that non-specific labelling almost did not occur. This approach has already been acknowledged as a useful tool to assess the specific and selective attachment of target molecules for sensoring purposes (Daniel J. Thomas et al., 2014).

Overall, the combined information of FTIR and RAMAN spectra, the electron microscopy images and confocal microscopy photographs confirmed the successful formation of NIP and MIP films and the ability of MIP film to rebind selectively and sensitively to its target compound.

3.4 Performance of MIP sensor

3.4.1 Calibration curve

The analytical performance of 8-OHdG sensory materials was evaluated by recording calibration curves. Figures 6A-B presents EIS calibration curves plotted with the R_{ct} of MIP and NIP sensors against the logarithm concentration of 8-OHdG. For each calibration study, sensors were previously

incubated in PBS solution until a stable response was obtained. Afterwards, the time given for 8-OHdG incubation was set to 20 min.

In order to evaluate the specificity and selectivity of the assembled biosensors, the value of the imprinting factor (IF = [*template rebound by MIP*] / [*template rebound by NIP*]) can be used as a comparative tool. From the ratio of sensitivity of the MIP sensor to 8-OHdG and to the NIP one, the IF was determined to be ~6.3.

The results obtained demonstrated that the resistance of the sensing layer increased after incubating an 8-OHdG solution in the MIP film, which could be due to the re-binding of 8-OHdG onto the imprinted cavities that hindered the electrical features of the sensing surface $[Fe(CN)_6]^{3-/4-}$. In general, increasing concentrations of 8-OHdG increased the diameter of the semicircles in the Nyquist plot (R_{ct}), indicating that 8-OHdG bound to the sensory layer increased the charge-transfer resistance of the probe. The calibration curve obtained for the MIP sensor showed a linear relationship over 8-OHdG concentration in the range [0.1−100] pg/ml. The limit of detection (*LOD*), was 0.74 pg/ml, calculated by extracting the first standard from the calibration curve and extending the linear ranges observed, as in potentiometric devices that respond to concentration in a logarithm basis. The response of the control electrode (NIP) was independent of the 8-OHdG concentration and it was kept at very low values for all concentrations within that range (random and small R_{ct} values). All the results were normalized against the blank value (PBS). Furthermore, the reproducibility of the sensors for quantification of 8-OHdG was investigated over the entire linear range and the results showed that the relative standard deviation (RSD) was 0.5-8.8 %.

3.4.2 Selectivity studies

Uric acid is typically identified as the major electrochemical interfering species in biological samples, mainly due to its relatively high concentrations, and, here specifically, the similar structural characteristics to the 8-OHdG molecule. Therefore, in order to verify the selectivity of the sensory

device, uric acid, citric acid and glucose were selected as interfering species. Data presented on figure S2 showed that these molecules almost have no interference in the determination of 8-OHdG, showing variations of 3.0, 12.0 and 0.5% for uric acid, citric acid and glucose, respectively. Moreover, to assess its effect upon the biosensor response, the calibration curves were performed directly in human urine samples (uric acid levels of ~500 ug/ml). EIS calibration curves against 8-OHdG concentration for MIP and NIP sensors are presented in Figure 6C. It was interesting to observe that the MIP maintained the linear EIS response over the considered concentration range, with just a small decrease of the sensitivity. In contrast, the NIP sensor presented a quite random behaviour which can be a strong indication that its response is caused by non-specific adsorption at the electrode modified-surface. Thus, the proposed sensor showed good analytical performance in terms of sensitivity, selectivity and rapid response towards 8-OHdG determination.

3.4.3 Analysis of spiked human urine samples

Urine samples were assayed and recovery experiments were carried out via the standard addition method by adding 0.25, 2.5 and 50 pg/ml. Assuming a null concentration of the urine sample (because it was used as background media for the overall calibration), the obtained recovery values were of 92.6, 111.6 and 110.3%, respectively. But, in biological samples 8-OHdG molecule is present in vestigial levels and so, herein, we also estimated this "background concentration". Thus, we have employed the Gran's method of multiple standard addition to estimate the original concentration of the 8-OHdG in urine samples (Galvis-Sanchez, Santos, & Rangel, 2015). As can be seen in Figure S3, the plot of $10^{(\text{Rct relative/Slope})}$ *versus* the concentration of 8-OHdG (added) results in a linear behaviour where the *x* axis interception is a direct indication of the unknown 8-OHdG concentration initially present in the urine real sample (before spiking). The calculated 8-OHdG concentration in the real urine sample (before 1:1000 dilution) was 4.1 ng/ml, a value that still is below the maximum limit in healthy humans.

Overall, these results demonstrated that the method was suitable for the determination of the total content of 8-OHdG in urine samples. Although there are already few researches on the application of sensitive sensors for detection of 8-OHdG, they often require the sample pre-treating stages to eliminate the presence of interfering species (Jia et al., 2015).

4. Conclusions

In the present study, an electropolymerization method was selected for the synthesis of a MIP-based electrochemical sensor targeted for 8-OHdG recognition and detection. Under this approach, phenol was electrochemically deposited on gold-modified electrodes in the presence of the template molecule 8-OHdG. The control of some experimental parameters of the electropolymerization reaction enabled the preparation of thin homogenous films, which constitute an important issue in order to achieve trustable, accurate and repeatable sensor responses. Our results demonstrated that 8-OHdG molecule was successfully entrapped into the polymeric matrix, enabling a three-dimensional structure with numerous imprinted cavities sites. The developed electrochemical biosensor showed high sensitivity and selectivity towards 8-OHdG over the wide concentration range. The successful application of the proposed sensor in the analysis of human urine samples has evidenced its promising features in the early diagnosis of cancer in point-of-care.

Overall, a simple and easy-to-go detection method of 8-OHdG in biological samples was possible without any previous sample preparation, providing a great advantage for this new analytical methodology. Compared to previous methods (table S1), the work described herein showed the best lower limit of linear range and limit of detection, coupled with a wide range of concentrations of linear response.

5. Acknowledgements

This research was supported by Portuguese Foundation for Science and Technology (FCT) (*PhD Grant reference SFRH/BD/94159/2013*) and was partially financed by FEDER funds through the COMPETE 2020 Programme and National Funds under the project UID/CTM/50025/2013.

6. References

Alvarez-Lorenzo, C., & Concheiro, A. (2004). Molecularly imprinted polymers for drug delivery. *Journal of Chromatography B: Analytical Technologies in the Biomedical and Life Sciences*, *804*, 231–245.

Arnett, S. D., Osbourn, D. M., Moore, K. D., Vandaveer, S. S., & Lunte, C. E. (2005). Determination of 8-oxoguanine and 8-hydroxy-2'-deoxyguanosine in the rat cerebral cortex using microdialysis sampling and capillary electrophoresis with electrochemical detection. *Journal of Chromatography. B, Analytical Technologies in the Biomedical and Life Sciences*, *827*(1), 16–25.

Barde, L. N., Ghule, M. M., Roy, A. a., Mathur, V. B., & Shivhare, U. D. (2012). Development of molecularly imprinted polymer as sustain release drug carrier for propranolol HCL. *Drug Development and Industrial Pharmacy*, *39*, 1–7.

Blanco-López, M. C., Lobo-Castañón, M. J., Miranda-Ordieres, J., & Tuñón-Blanco, P. (2003). Voltammetric sensor for vanillylmandelic acid based on molecularly imprinted polymer-modified electrodes. *Biosensors & Bioelectronics*, *18*(4), 353–62.

Bolner, A., Pilleri, M., Riva, V. D. E., & Nordera, G. P. (2011). Plasma and Urinary HPLC-ED Determination of the Ratio of 8-OHdG / 2-dG in Parkinson' s Disease. *Clin. Lab.*, 859–866.

Daniel J. Thomas, Zari Tehrani, & Mohd Azraie B. Mohd Azmi. (2014). Silicon nanowire immunosensor for detection of 8-hydroxy-2′-deoxyguanosine oxidative stress cancer biomarker. *Journal of Surface Science and Nanotechnology*, *12*, 349–357.

de Zwart, L. L., Meerman, J. H. ., Commandeur, J. N. ., & Vermeulen, N. P. . (1999). Biomarkers of free radical damage. *Free Radical Biology and Medicine*, *26*(98), 202–226.

Ferreira, M., Varela, H., Torresi, R. M., & Tremiliosi-Filho, G. (2006). Electrode passivation caused by polymerization of different phenolic compounds. *Electrochimica Acta*, *52*(2), 434–442.

Ferreira, N. S., & Sales, M. G. F. (2014). Disposable immunosensor using a simple method for oriented antibody immobilization for label-free real-time detection of an oxidative stress biomarker implicated in cancer diseases. *Biosensors & Bioelectronics*, *53*, 193–9.

Frenkel, K. (1992). Carcinogen-mediated oxidant formation and oxidative DNA damage. *Pharmacology and Therapeutics*, *53*, 127–166.

Galvis-Sanchez, A. C., Santos, J. R., & Rangel, A. O. S. S. (2015). Standard addition flow method for potentiometric measurements at low concentration levels: Application to the determination of fluoride in food samples. *Talanta*, *133*, 1–6.

Gohary, N. A. El, Madbouly, A., Nashar, R. M. El, & Mizaikoff, B. (2014). Synthesis and application of a molecularly imprinted polymer for the voltammetric determination of famciclovir. *Biosensors and Bioelectronics*, *65C*.

Guan, Y., Zhou, G., & Ye, J. (2014). Fast Quantification of Salivary 8-Hydroxy-2′-deoxyguanosine as DNA Damage Biomarker Using CE with Electrochemical Detection. *Chromatographia*, *77*(7-8), 603–607.

Guo, H., Xue, K., & Yan, L. (2012). Resonance Rayleigh scattering spectral method for determination of urinary 8-hydroxy-2′-deoxyguanosine using gold nanoparticles as probe. *Sensors and Actuators B: Chemical*, *171-172*, 1038–1045.

Gupta, P., Oyama, M., & Goyal, R. N. (2016). Electrochemical investigations of 8-hydroxydeoxyguanosine and its determination at an edge plane pyrolytic graphite electrode.

RSC Adv., *6*(3), 1722–1728.

Gutiérrez, A., Gutierrez, F., Eguílaz, M., González-Domínguez, J. M., Hernández-ferrer, J., Ansón-casaos, A., Rivas, G. (2016). Electrochemical sensing of guanine, adenine and 8-hydroxy-2′-deoxyguanosine at glassy carbon modified with single-walled carbon nanotubes covalently functionalized with lysine. *RSC Adv.*, *6*, 13469–13477.

Gutiérrez, A., Osegueda, S., Gutiérrez-Granados, S., Alatorre, A., García, M. G., & Godínez, L. A. (2008). Amperometric Detection and Quantification of 8-Hydroxy-2′-deoxyguanosine (8-OHdG) Using Dendrimer Modified Electrodes. *Electroanalysis*, *20*(21), 2294–2300.

Hawkins, D. M., Trache, A., Ellis, E. A., Stevenson, D., Holzenburg, A., Meininger, G. a., & Reddy, S. M. (2006). Quantification and confocal imaging of protein specific molecularly imprinted polymers. *Biomacromolecules*, *7*(9), 2560–2564.

Huang, J., Xing, X., Zhang, X., He, X., Lin, Q., Lian, W., & Zhu, H. (2011). A molecularly imprinted electrochemical sensor based on multiwalled carbon nanotube-gold nanoparticle composites and chitosan for the detection of tyramine. *Food Research International*, *44*(1), 276–281.

Jia, L., & Wang, H. (2013). Electrochemical reduction synthesis of graphene/Nafion nanocomposite film and its performance on the detection of 8-hydroxy-2’-deoxyguanosine in the presence of uric acid. *Journal of Electroanalytical Chemistry*, *705*, 37–43.

Jia, L.-P., Liu, J.-F., & Wang, H.-S. (2015). Electrochemical performance and detection of 8-Hydroxy-2′-deoxyguanosine at single-stranded DNA functionalized graphene modified glassy carbon electrode. *Biosensors and Bioelectronics*, *67*, 139–145.

Kamel, A. H., Moreira, F. T. C., Delerue-Matos, C., & Sales, M. G. F. (2008). Electrochemical determination of antioxidant capacities in flavored waters by guanine and adenine biosensors. *Biosensors & Bioelectronics*, *24*(4), 591–9.

Kasai, H. (1997). Analysis of a form of oxidative DNA damage , 8-hydroxy-2'-deoxyguanosine , as a marker of cellular oxidative stress during carcinogenesis. *Mutation Research, 387(3), 147-163.*

Lapuente, R., Cases, F., & Garce, P. (1998). A voltammetric and FTIR – ATR study of the electropolymerization of phenol on platinum electrodes in carbonate medium Influence of sulfide. *Journal of Electroanalytical Chemistry*, *451*, 163–171.

Lee, K.-H., Shu, X.-O., Gao, Y.-T., Ji, B.-T., Yang, G., Blair, A., Kang, D. (2010). Breast cancer and urinary biomarkers of polycyclic aromatic hydrocarbon and oxidative stress in the Shanghai Women's Health Study. *Cancer Epidemiology, Biomarkers & Prevention : A Publication of the American Association for Cancer Research, Cosponsored by the American Society of Preventive Oncology*, *19*(3), 877–83.

Li, L., Yang, L., Xing, Z., Lu, X., & Kan, X. (2013). Surface molecularly imprinted polymers-based electrochemical sensor for bovine hemoglobin recognition. *The Analyst*, *138*, 6962–8.

Li, T. H., Jia, W. L., Wang, H. S., & Liu, R. M. (2007). Electrochemical performance of 8-hydroxy-2'-deoxyguanosine and its detection at poly(3-methylthiophene) modified glassy carbon electrode. *Biosensors and Bioelectronics*, *22*, 1245–1250.

Liu, B., Lian, H. T., Yin, J. F., & Sun, X. Y. (2012). Dopamine molecularly imprinted electrochemical sensor based on graphene–chitosan composite. *Electrochimica Acta*, *75*, 108–114.

Luo, J., Jiang, S., & Liu, X. (2014). Electrochemical sensor for bovine hemoglobin based on a novel graphene-molecular imprinted polymers composite as recognition element. *Sensors and Actuators B: Chemical*, *203*, 782–789.

Malitesta, C., Mazzotta, E., Picca, R. a, Poma, A., Chianella, I., & Piletsky, S. a. (2012). MIP sensors--the electrochemical approach. *Analytical and Bioanalytical Chemistry*, *402*(5), 1827–46.

Mei, S., Yao, Q., Wu, C., & Xu, G. (2005). Determination of urinary 8-hydroxy-2'-deoxyguanosine by two approaches - Capillary electrophoresis and GC/MS: An assay for in vivo oxidative DNA damage in cancer patients. *Journal of Chromatography B: Analytical Technologies in the Biomedical and Life Sciences*, *827*, 83–87.

Mohd Azmi, M. a, Tehrani, Z., Lewis, R. P., Walker, K. D., Jones, D. R., Daniels, D. R., Guy, O. J. (2014). Highly sensitive covalently functionalised integrated silicon nanowire biosensor devices for detection of cancer risk biomarker. *Biosensors & Bioelectronics*, *52*, 216–24.

Moreira, F. T. C., Dutra, R. a. F., Noronha, J. P. C., Fernandes, J. C. S., & Sales, M. G. F. (2013). Novel biosensing device for point-of-care applications with plastic antibodies grown on Au-screen printed electrodes. *Sensors and Actuators B: Chemical*, *182*, 733–740.

Moreira, F. T. C., Sharma, S., Dutra, R. a F., Noronha, J. P. C., Cass, A. E. G., & Sales, M. G. F. (2013). Smart plastic antibody material (SPAM) tailored on disposable screen printed electrodes for protein recognition: application to myoglobin detection. *Biosensors & Bioelectronics*, *45*, 237–44.

Nguyen, T. H., & Ansell, R. J. (2009). Fluorescent imprinted polymer sensors for chiral amines. *Organic & Biomolecular Chemistry*, *7*(6), 1211–20.

Owens, P. K., Karlsson, L., Lutz, E. S. M., & Andersson, L. I. (1999). Molecular imprinting for bio- and pharmaceutical analysis. *TrAC - Trends in Analytical Chemistry*, *18*(3), 146–154.

Pan, D., Zhou, Q., Rong, S., Zhang, G., Zhang, Y., Liu, F., Pan, H. (2016). Electrochemical immunoassay for the biomarker 8-hydroxy-2′-deoxyguanosine using a glassy carbon electrode modified with chitosan and poly(indole-5-carboxylic acid). *Microchimica Acta*, *183*(1), 361–368.

Panasyuk, T. L., Mirsky, V. M., Piletsky, S. A., & Wolfbeis, O. S. (1999). Electropolymerized Molecularly Imprinted Polymers as Receptor Layers in Capacitive Chemical Sensors. *Anal.*

Chem., *71*(20), 4609–4613.

Pernites, R., Ponnapati, R., Felipe, M. J., & Advincula, R. (2011). Electropolymerization molecularly imprinted polymer (E-MIP) SPR sensing of drug molecules: pre-polymerization complexed terthiophene and carbazole electroactive monomers. *Biosensors & Bioelectronics*, *26*(5), 2766–71.

Repine JE, Bast A, L. I. (1997). State of the Art Oxidative Stress in Chronic Obstructive. *American Journal of Respiratory and Critical Care Medicine*, *156*(10), 341–57.

Richard G. Cutler, H. R. (2002). Critical Reviews of Oxidative Stress and Aging: Advances in Basic Science, Diagnostics and Intervention. In *Critical Reviews of Oxidative Stress and Aging Advances in Basic Science, Diagnostics and Intervention*, *2*, 1–1624.

Riskin, M., Tel-Vered, R., & Willner, I. (2007). The Imprint of Electropolymerized Polyphenol Films on Electrodes by Donor-Acceptor Interactions: Selective Electrochemical Sensing of N,N′-dimethyl-4,4′-bipyridinium (Methyl Viologen). *Advanced Functional Materials*, *17*(18), 3858–3863.

Sahebnasagh, A., Karimi, G., & Mohajeri, S. A. (2014). Preparation and Evaluation of Histamine Imprinted Polymer as a Selective Sorbent in Molecularly Imprinted Solid-Phase Extraction Coupled with High Performance Liquid Chromatography Analysis in Canned Fish. *Food Analytical Methods*, *7*, 1–8.

Say, R., Gültekin, A., Ozcan, A. A., Denizli, A., & Ersöz, A. (2009). Preparation of new molecularly imprinted quartz crystal microbalance hybride sensor system for 8-hydroxy-2'-deoxyguanosine determination. *Analytica Chimica Acta*, *640*(1-2), 82–6.

Sharma, P. S., Pietrzyk-Le, A., D'Souza, F., & Kutner, W. (2012). Electrochemically synthesized polymers in molecular imprinting for chemical sensing. *Analytical and Bioanalytical Chemistry*, *402*(10), 3177–204.

Shen, Q., & Wang, X. (2009). Simultaneous determination of adenine, guanine and thymine based on β-cyclodextrin/MWNTs modified electrode. *Journal of Electroanalytical Chemistry*, *632*(1-2), 149–153.

Socrates, G. (2004). *Infrared and Raman Characteristic Group Frequencies*.

Subash, P., Gurumurthy, P., Sarasabharathi, a, & Cherian, K. M. (2010). Urinary 8-OHdG: A marker of oxidative stress to DNA and total antioxidant status in essential hypertension with South Indian population. *Indian Journal of Clinical Biochemistry : IJCB*, *25*(2), 127–32.

Tehrani, Z., Burwell, G., Azmi, M. a M., Castaing, a, Rickman, R., Almarashi, J., Guy, O. J. (2014). Generic epitaxial graphene biosensors for ultrasensitive detection of cancer risk biomarker. *2D Materials*, *25004*.

Valavanidis, A., Vlachogianni, T., & Fiotakis, C. (2009). 8-hydroxy-2'-deoxyguanosine (8-OHdG): A critical biomarker of oxidative stress and carcinogenesis. *Journal of Environmental Science and Health. Part C, Environmental Carcinogenesis & Ecotoxicology Reviews*, *27*(2), 120–39.

Vallano, P. T., & Remcho, V. T. (2000). Highly selective separations by capillary electrochromatography: Molecular imprint polymer sorbents. *Journal of Chromatography A*, *887*, 125–135.

Wang, J. C., Wang, Y. S., Xue, J. H., Zhou, B., Qian, Q. M., Wang, Y. S., Liu, S. Du. (2014). An ultrasensitive label-free assay of 8-hydroxy-2'-deoxyguanosine based on the conformational switching of aptamer. *Biosensors and Bioelectronics*, *58*, 22–26.

Wang, Z., Kang, J., Liu, X., & Ma, Y. (2007). Capacitive Detection of Theophylline Based on Electropolymerized Molecularly Imprinted Polymer. *International Journal of Polymer Analysis and Characterization*, *12*, 131–142.

Whitcombe, M. J., Chianella, I., Larcombe, L., Piletsky, S. a, Noble, J., Porter, R., & Horgan, A.

(2011). The rational development of molecularly imprinted polymer-based sensors for protein detection. *Chemical Society Reviews*, *40*, 1547–1571.

Yang, L., Wang, B., Qi, H., Gao, Q., Li, C., & Zhang, C. (2015). Highly Sensitive Electrochemical Sensor for the Determination of 8-Hydroxy-2 '-deoxyguanosine Incorporating SWCNTs-Nafion Composite Film, *2015*,1-11.

Yang, Y., Yi, C., Luo, J., Liu, R., Liu, J., Jiang, J., & Liu, X. (2011). Glucose sensors based on electrodeposition of molecularly imprinted polymeric micelles: a novel strategy for MIP sensors. *Biosensors & Bioelectronics*, *26*(5), 2607–12.

Yano, T., Shoji, F., Baba, H., Koga, T., Shiraishi, T., Orita, H., & Kohno, H. (2009). Significance of the urinary 8-OHdG level as an oxidative stress marker in lung cancer patients. *Lung Cancer*, *63*, 111–114.

Yola, M. L., Eren, T., & Atar, N. (2015). A sensitive molecular imprinted electrochemical sensor based on gold nanoparticles decorated graphene oxide: Application to selective determination of tyrosine in milk. *Sensors and Actuators B: Chemical*, *210*, 149–157.

Zhang, T.-T., Zhao, H.-M., Fan, X.-F., Chen, S., & Quan, X. (2015). Electrochemiluminescence immunosensor for highly sensitive detection of 8-hydroxy-2′-deoxyguanosine based on carbon quantum dot coated Au/SiO2 core–shell nanoparticles. *Talanta*, *131*, 379–385.

Figure Captions:

Figure 1. *Schematic representation of the assembly of the gold-modified imprinted sensor.*

Figure 2. A) *Cyclic voltammograms of a gold-modified electrode immersed in 0.01 M PBS aqueous solution containing different concentrations of monomer phenol (0.25, 0.5 and 1.25 mM), pH 7.4, scan rate 20 mVs^{-1};* ***B)*** *Charge variation during electropolymerization of phenol (3 cycles) obtained from MIPs with different ratios of template to monomer (1:3 and 1:1) and NIP in 0.01 M PBS and* ***C)*** *Cyclic voltammograms concerning the electropolymerization of 0.25 mM phenol in 0.01 M PBS, pH*

7.4, (scan rate 20 mVs^{-1}, 3 cycles) at gold-modified electrodes with (dashed line) and without (straight line) the template molecule 8-OHdG.

Figure 3. A) *CV of the gold electrode (green line), thiol-modified gold electrode (red line), NIP and MIP after electropolymerization (blue and grey line, respectively) and after template removal (black lines, on the right side), measured in aqueous solution containing 5 mM $[Fe(CN)_6]^{3-/4-}$ in 0.01 M PBS pH 7.4 and* ***B)*** *EIS of (a) gold electrode, (b) thiol-modified gold electrode, NIP (c) before and (d) after removal, MIP (e) before and (f) after removal, in aqueous solution containing 5 mM $[Fe(CN)_6]^{3-/4-}$ in 0.01 M PBS.*

Figure 4. A) *FTIR-ATR spectra of gold, thiol-modified gold, NIP and MIP electrodes;* ***B)*** *RAMAN spectra of gold, thiol-modified gold, NIP and MIP electrodes and* ***C)*** *typical image from RAMAN, measured at 50x magnification, of the gold-screen printed electrodes (Au-SPE).*

Figure 5. A) *SEM micrographs of NIP and MIP electrodes and* ***B)*** *confocal imaging of FITC antibody against 8-OHdG attached to NIP and MIP surfaces.*

Figure 6. A) *Nyquist plot of MIP sensor in 5 mM $[Fe(CN)_6]^{3-/4-}$ in 0.01 M PBS pH 7.4, previously incubated in increasing concentrations of 8-OHdG and* ***B)*** *the corresponding calibration curves for both MIP and NIP sensors;* ***C)*** *Calibration curves of NIP and MIP sensors for different 8-OHdG concentrations in urine samples, measured in 5 mM $[Fe(CN)_6]^{3-/4-}$ in 0.01 M PBS pH 7.4. All error bars represent the standard deviation for three independent measurements.*

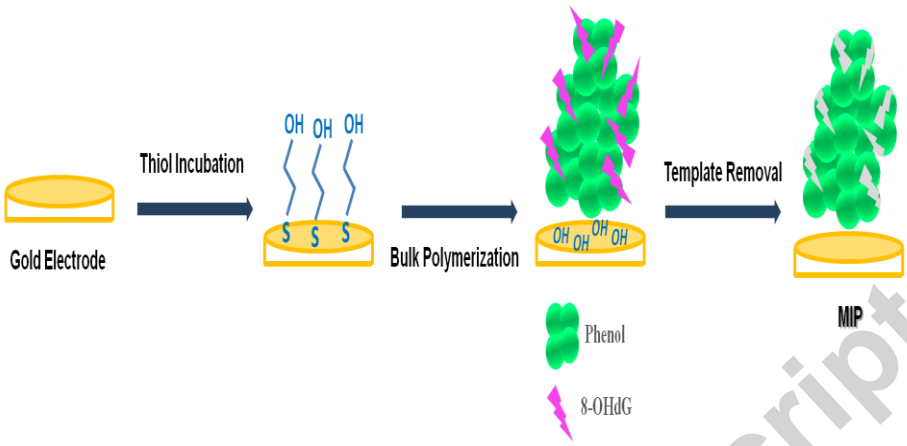

Figure 1

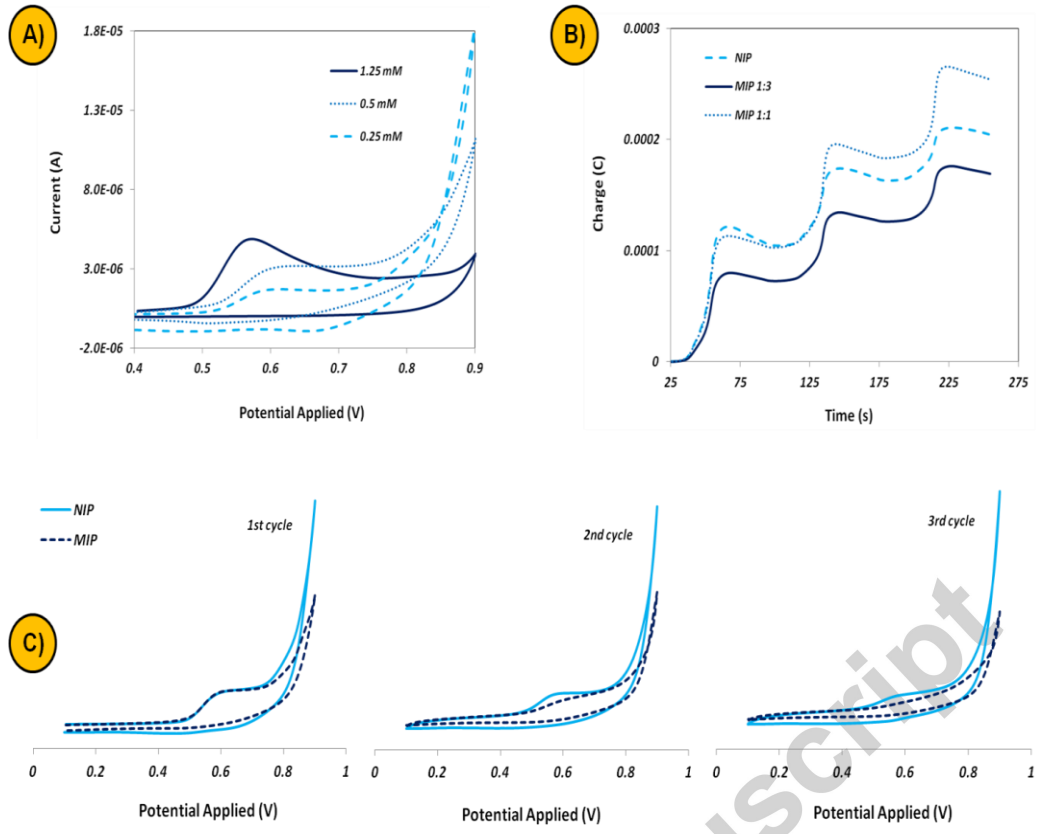

Figure 2

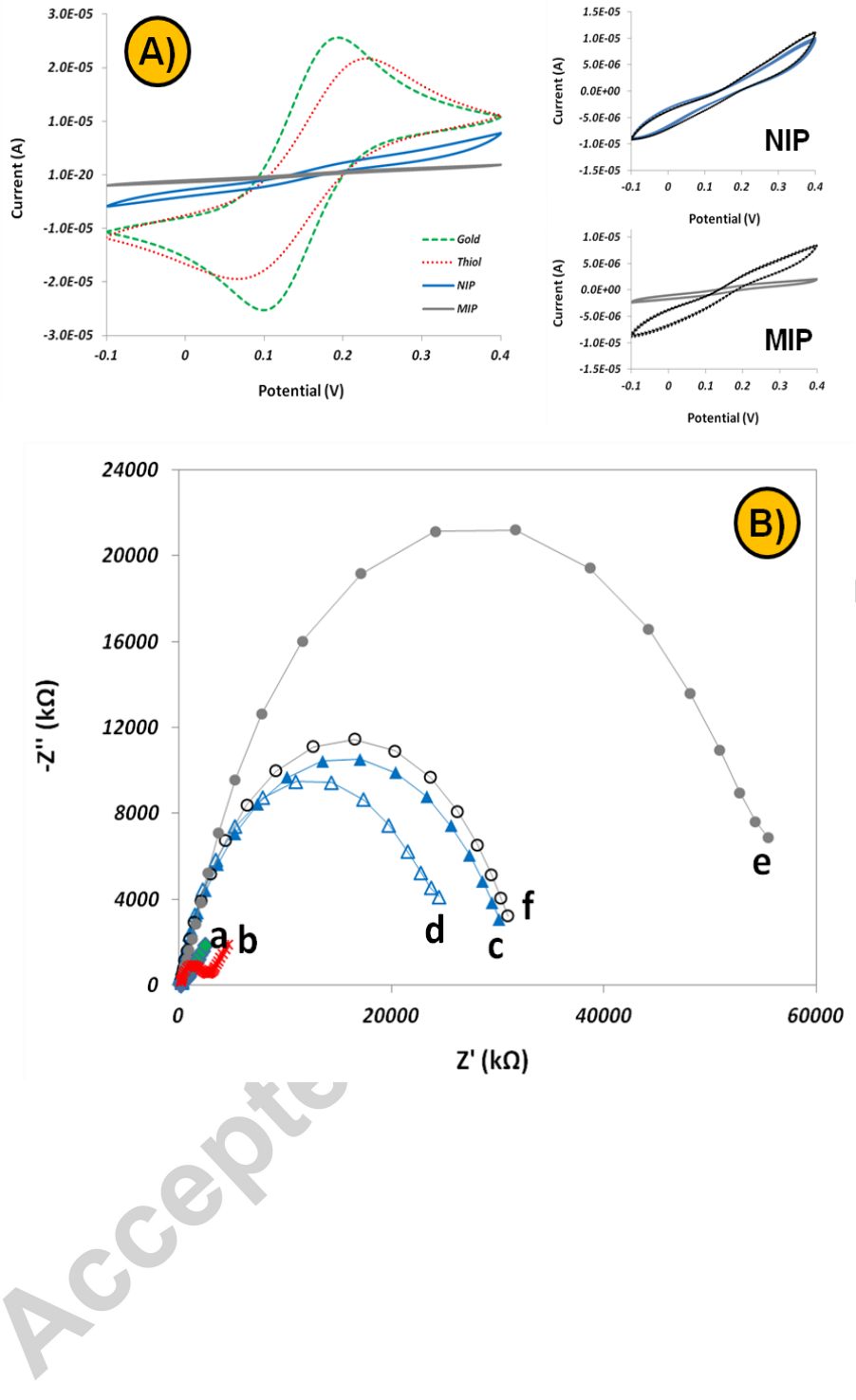

Figure 3

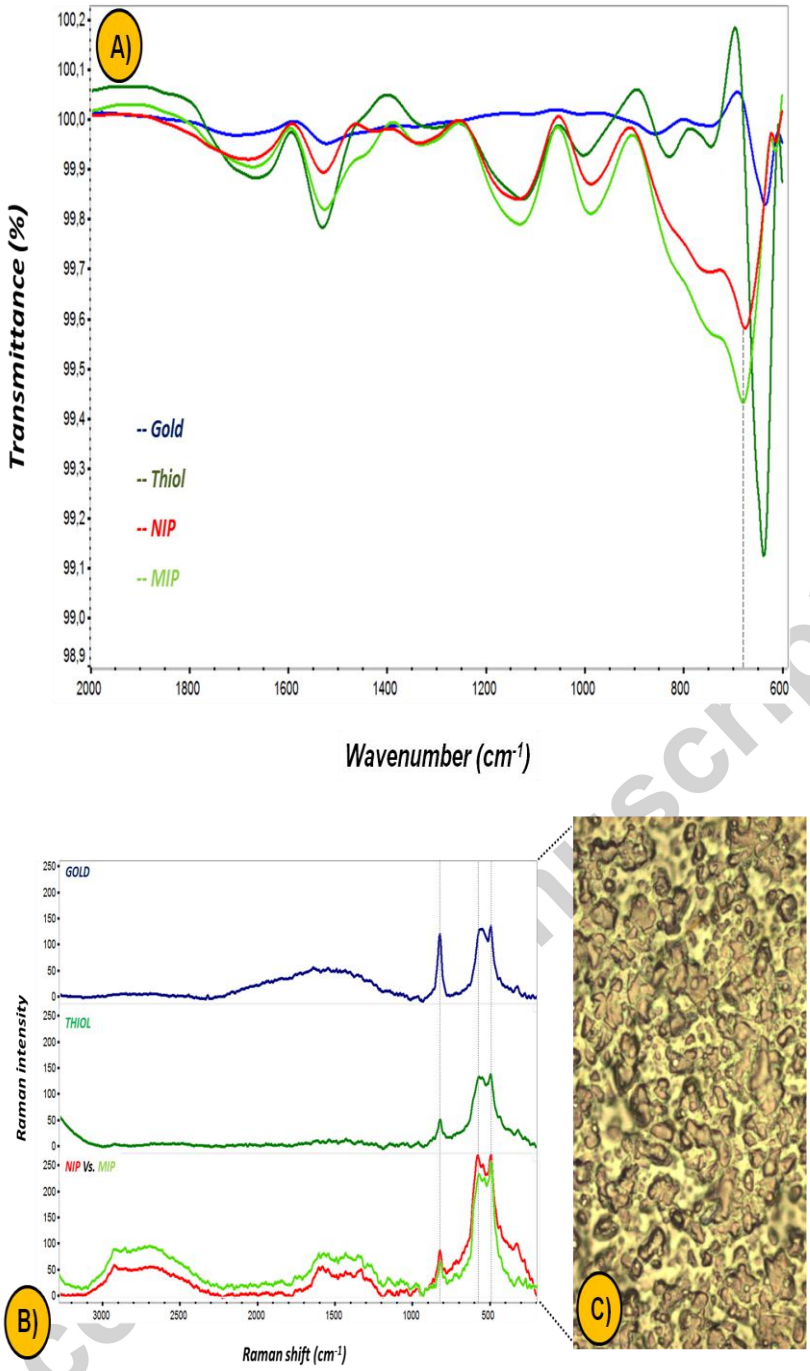

Figure 4

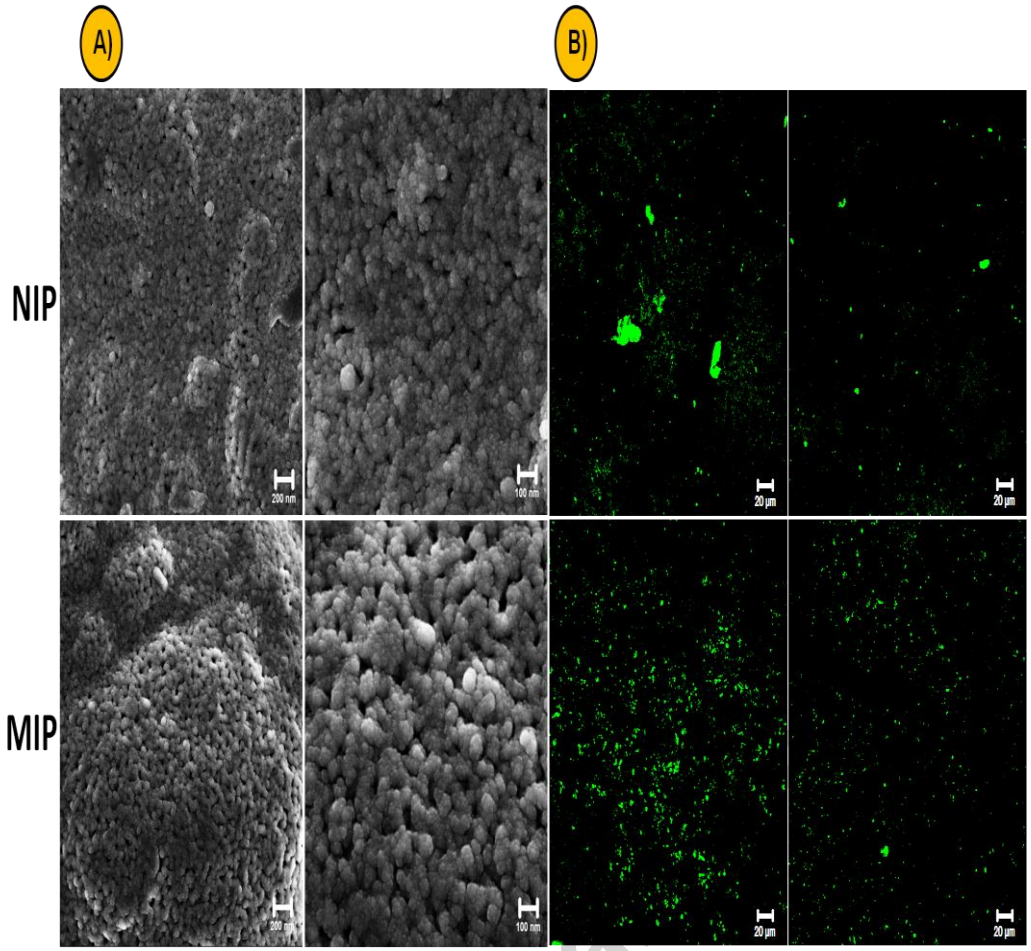

Figure 5

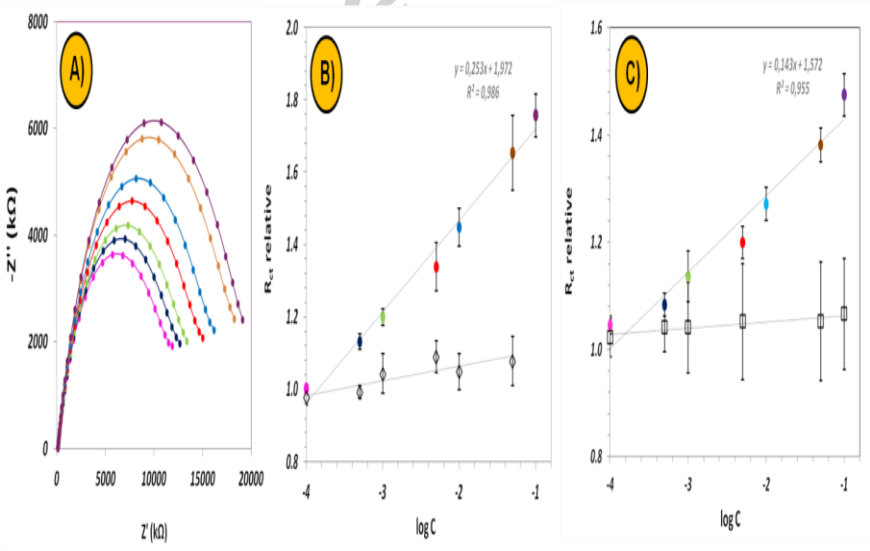

Figure 6

Highlights

- Simple and straightforward *in-situ* biosensor design
- Imprinted sensing layer produced *on-site* by electropolymerization
- Phenol monomer base electropolymerization
- Detection of an oxidative stress biomarker, 8-hydroxy-2'-deoxyguanosine
- Detection of the biomarker in human urine samples